

Properties of Jets in Z Boson Events from 1.8 TeV $\bar{p}p$ Collisions

F. Abe,¹⁴ H. Akimoto,³² A. Akopian,²⁷ M.G. Albrow,⁷ S.R. Amendolia,²³ D. Amidei,¹⁷
 J. Antos,²⁹ C. Anway-Wiese,⁴ S. Aota,³² G. Apollinari,²⁷ T. Asakawa,³² W. Ashmanskas,¹⁵
 M. Atac,⁷ F. Azfar,²² P. Azzi-Bacchetta,²¹ N. Bacchetta,²¹ W. Badgett,¹⁷ S. Bagdasarov,²⁷
 M. W. Bailey,¹⁹ J. Bao,³⁵ P.de Barbaro,²⁶ A. Barbaro-Galtieri,¹⁵ V.E. Barnes,²⁵
 B.A. Barnett,¹³ E. Barzi,⁸ G. Bauer,¹⁶ T. Baumann,⁹ F. Bedeschi,²³ S. Behrends,³
 S. Belforte,²³ G. Bellettini,²³ J. Bellinger,³⁴ D. Benjamin,³¹ J. Benloch,¹⁶ J. Bensinger,³
 D. Benton,²² A. Beretvas,⁷ J.P. Berge,⁷ J. Berryhill,⁵ S. Bertolucci,⁸ A. Bhatti,²⁷
 K. Biery,¹² M. Binkley,⁷ D. Bisello,²¹ R.E. Blair,¹ C. Blocker,³ A. Bodek,²⁶ W. Bokhari,¹⁶
 V. Bolognesi,⁷ D. Bortoletto,²⁵ J. Boudreau,²⁴ L. Breccia,² C. Bromberg,¹⁸ N. Bruner,¹⁹
 E. Buckley-Geer,⁷ H.S. Budd,²⁶ K. Burkett,¹⁷ G. Busetto,²¹ A. Byon-Wagner,⁷
 K.L. Byrum,¹ J. Cammerata,¹³ C. Campagnari,⁷ M. Campbell,¹⁷ A. Caner,⁷
 W. Carithers,¹⁵ D. Carlsmith,³⁴ A. Castro,²¹ D. Cauz,²³ Y. Cen,²⁶ F. Cervelli,²³
 P.S. Chang,²⁹ P.T. Chang,²⁹ H.Y. Chao,²⁹ J. Chapman,¹⁷ M.-T. Cheng,²⁹ G. Chiarelli,²³
 T. Chikamatsu,³² C.N. Chiou,²⁹ L. Christofek,¹¹ S. Cihangir,⁷ A.G. Clark,²³ M. Cobal,²³
 M. Contreras,⁵ J. Conway,²⁸ J. Cooper,⁷ M. Cordelli,⁸ C. Couyoumtzelis,²³ D. Crane,¹
 D. Cronin-Hennessy,⁶ R. Culbertson,⁵ J.D. Cunningham,³ T. Daniels,¹⁶ F. DeJongh,⁷
 S. Delchamps,⁷ S. Dell'Agnello,²³ M. Dell'Orso,²³ L. Demortier,²⁷ B. Denby,²³ M. Deninno,²
 P.F. Derwent,¹⁷ T. Devlin,²⁸ J.R. Dittmann,⁶ S. Donati,²³ J. Done,³⁰ T. Dorigo,²¹
 A. Dunn,¹⁷ N. Eddy,¹⁷ K. Einsweiler,¹⁵ J.E. Elias,⁷ R. Ely,¹⁵ E. Engels, Jr.,²⁴ D. Errede,¹¹
 S. Errede,¹¹ Q. Fan,²⁶ I. Fiori,² B. Flaughner,⁷ G.W. Foster,⁷ M. Franklin,⁹ M. Frautschi,³¹
 J. Freeman,⁷ J. Friedman,¹⁶ H. Frisch,⁵ T.A. Fuess,¹ Y. Fukui,¹⁴ S. Funaki,³²
 G. Gagliardi,²³ S. Galeotti,²³ M. Gallinaro,²¹ M. Garcia-Sciveres,¹⁵ A.F. Garfinkel,²⁵
 C. Gay,⁹ S. Geer,⁷ D.W. Gerdes,¹⁷ P. Giannetti,²³ N. Giokaris,²⁷ P. Giromini,⁸
 L. Gladney,²² D. Glenzinski,¹³ M. Gold,¹⁹ J. Gonzalez,²² A. Gordon,⁹ A.T. Goshaw,⁶
 K. Goulios,²⁷ H. Grassmann,²³ L. Groer,²⁸ C. Grosso-Pilcher,⁵ G. Guillian,¹⁷ R.S. Guo,²⁹
 C. Haber,¹⁵ E. Hafen,¹⁶ S.R. Hahn,⁷ R. Hamilton,⁹ R. Handler,³⁴ R.M. Hans,³⁵ K. Hara,³²
 A.D. Hardman,²⁵ B. Harral,²² R.M. Harris,⁷ S.A. Hauger,⁶ J. Hauser,⁴ C. Hawk,²⁸
 E. Hayashi,³² J. Heinrich,²² K.D. Hoffman,²⁵ M. Hohlmann,^{1,5} C. Holck,²² R. Hollebeek,²²
 L. Holloway,¹¹ A. Holscher,¹² S. Hong,¹⁷ G. Houk,²² P. Hu,²⁴ B.T. Huffman,²⁴ R. Hughes,²⁶
 J. Huston,¹⁸ J. Huth,⁹ J. Hylen,⁷ H. Ikeda,³² M. Incagli,²³ J. Incandela,⁷ G. Introzzi,²³
 J. Iwai,³² Y. Iwata,¹⁰ H. Jensen,⁷ U. Joshi,⁷ R.W. Kadel,¹⁵ E. Kajfasz,^{7a} T. Kamon,³⁰
 T. Kaneko,³² K. Karr,³³ H. Kasha,³⁵ Y. Kato,²⁰ T.A. Keaffaber,²⁵ L. Keeble,⁸ K. Kelley,¹⁶
 R.D. Kennedy,²⁸ R. Kephart,⁷ P. Kesten,¹⁵ D. Kestenbaum,⁹ R.M. Keup,¹¹ H. Keutelian,⁷
 F. Keyvan,⁴ B. Kharadia,¹¹ B.J. Kim,²⁶ D.H. Kim,^{7a} H.S. Kim,¹² S.B. Kim,¹⁷ S.H. Kim,³²
 Y.K. Kim,¹⁵ L. Kirsch,³ P. Koehn,²⁶ K. Kondo,³² J. Konigsberg,⁹ S. Kopp,⁵ K. Kordas,¹²
 W. Koska,⁷ E. Kovacs,^{7a} W. Kowald,⁶ M. Krasberg,¹⁷ J. Kroll,⁷ M. Kruse,²⁵ T.
 Kuwabara,³² S.E. Kuhlmann,¹ E. Kuns,²⁸ A.T. Laasanen,²⁵ N. Labanca,²³ S. Lammel,⁷
 J.I. Lamoureux,³ T. LeCompte,¹¹ S. Leone,²³ J.D. Lewis,⁷ P. Limon,⁷ M. Lindgren,⁴
 T.M. Liss,¹¹ N. Lockyer,²² O. Long,²² C. Loomis,²⁸ M. Loreti,²¹ J. Lu,³⁰ D. Lucchesi,²³
 P. Lukens,⁷ S. Lusin,³⁴ J. Lys,¹⁵ K. Maeshima,⁷ A. Maghakian,²⁷ P. Maksimovic,¹⁶

M. Mangano,²³ J. Mansour,¹⁸ M. Mariotti,²¹ J.P. Marriner,⁷ A. Martin,¹¹
 J.A.J. Matthews,¹⁹ R. Mattingly,¹⁶ P. McIntyre,³⁰ P. Melese,²⁷ A. Menzione,²³ E. Meschi,²³
 S. Metzler,²² C. Miao,¹⁷ G. Michail,⁹ R. Miller,¹⁸ H. Minato,³² S. Miscetti,⁸ M. Mishina,¹⁴
 H. Mitsuhashi,³² T. Miyamoto,³² S. Miyashita,³² Y. Morita,¹⁴ J. Mueller,²⁴ A. Mukherjee,⁷
 T. Muller,⁴ P. Murat,²³ H. Nakada,³² I. Nakano,³² C. Nelson,⁷ D. Neuberger,⁴
 C. Newman-Holmes,⁷ M. Ninomiya,³² L. Nodulman,¹ S.H. Oh,⁶ K.E. Ohl,³⁵ T. Ohmoto,¹⁰
 T. Ohsugi,¹⁰ R. Oishi,³² M. Okabe,³² T. Okusawa,²⁰ R. Oliver,²² J. Olsen,³⁴ C. Pagliarone,²
 R. Paoletti,²³ V. Papadimitriou,³¹ S.P. Pappas,³⁵ S. Park,⁷ A. Parri,⁸ J. Patrick,⁷
 G. Pauletta,²³ M. Paulini,¹⁵ A. Perazzo,²³ L. Pescara,²¹ M.D. Peters,¹⁵ T.J. Phillips,⁶
 G. Piacentino,² M. Pillai,²⁶ K.T. Pitts,⁷ R. Plunkett,⁷ L. Pondrom,³⁴ J. Proudfoot,¹
 F. Ptohos,⁹ G. Punzi,²³ K. Ragan,¹² A. Ribon,²¹ F. Rimondi,² L. Ristori,²³
 W. J. Robertson,⁶ T. Rodrigo,^{7a} S. Rolli,²³ J. Romano,⁵ L. Rosenson,¹⁶ R. Roser,¹¹
 W.K. Sakumoto,²⁶ D. Saltzberg,⁵ A. Sansoni,⁸ L. Santi,²³ H. Sato,³² V. Scarpine,³⁰
 P. Schlabach,⁹ E.E. Schmidt,⁷ M.P. Schmidt,³⁵ A. Scribano,²³ S. Segler,⁷ S. Seidel,¹⁹
 Y. Seiya,³² G. Sganos,¹² A. Sgolacchia,² M.D. Shapiro,¹⁵ N.M. Shaw,²⁵ Q. Shen,²⁵
 P.F. Shepard,²⁴ M. Shimojima,³² M. Shochet,⁵ J. Siegrist,¹⁵ A. Sill,³¹ P. Sinervo,¹²
 P. Singh,²⁴ J. Skarha,¹³ K. Sliwa,³³ F.D. Snider,¹³ T. Song,¹⁷ J. Spalding,⁷ P. Sphicas,¹⁶
 F. Spinella,²³ M. Spiropulu,⁹ L. Spiegel,⁷ L. Stanco,²¹ J. Steele,³⁴ A. Stefanini,²³
 K. Strahl,¹² J. Strait,⁷ R. Ströhmer,⁹ D. Stuart,⁷ G. Sullivan,⁵ A. Soumarokov,²⁹
 K. Sumorok,¹⁶ J. Suzuki,³² T. Takada,³² T. Takahashi,²⁰ T. Takano,³² K. Takikawa,³²
 N. Tamura,¹⁰ F. Tartarelli,²³ W. Taylor,¹² P.K. Teng,²⁹ Y. Teramoto,²⁰ S. Tether,¹⁶
 D. Theriot,⁷ T.L. Thomas,¹⁹ R. Thun,¹⁷ M. Timko,³³ P. Tipton,²⁶ A. Titov,²⁷ S. Tkaczyk,⁷
 D. Toback,⁵ K. Tollefson,²⁶ A. Tollestrup,⁷ J. Tonnison,²⁵ J.F.de Troconiz,⁹ S. Truitt,¹⁷
 J. Tseng,¹³ N. Turini,²³ T. Uchida,³² N. Uemura,³² F. Ukegawa,²² G. Unal,²²
 S.C. van den Brink,²⁴ S. Vejcik, III,¹⁷ G. Velez,²³ R. Vidal,⁷ M. Vondracek,¹¹ D. Vucinic,¹⁶
 R.G. Wagner,¹ R.L. Wagner,⁷ J. Wahl,⁵ C. Wang,⁶ C.H. Wang,²⁹ G. Wang,²³ J. Wang,⁵
 M.J. Wang,²⁹ Q.F. Wang,²⁷ A. Warburton,¹² T. Watts,²⁸ R. Webb,³⁰ C. Wei,⁶ C. Wendt,³⁴
 H. Wenzel,¹⁵ W.C. Wester, III,⁷ A.B. Wicklund,¹ E. Wicklund,⁷ R. Wilkinson,²²
 H.H. Williams,²² P. Wilson,⁵ B.L. Winer,²⁶ D. Wolinski,¹⁷ J. Wolinski,¹⁸ X. Wu,²³
 J. Wyss,²¹ A. Yagil,⁷ W. Yao,¹⁵ K. Yasuoka,³² Y. Ye,¹² G.P. Yeh,⁷ P. Yeh,²⁹ M. Yin,⁶
 J. Yoh,⁷ C. Yosef,¹⁸ T. Yoshida,²⁰ D. Yovanovitch,⁷ I. Yu,³⁵ L. Yu,¹⁹ J.C. Yun,⁷
 A. Zanetti,²³ F. Zetti,²³ L. Zhang,³⁴ W. Zhang,²² B. Zou,⁶ and S. Zucchelli²

(CDF Collaboration)

¹ Argonne National Laboratory, Argonne, Illinois 60439

² Istituto Nazionale di Fisica Nucleare, University of Bologna, I-40126 Bologna, Italy

³ Brandeis University, Waltham, Massachusetts 02254

⁴ University of California at Los Angeles, Los Angeles, California 90024

⁵ University of Chicago, Chicago, Illinois 60637

⁶ Duke University, Durham, North Carolina 27708

⁷ Fermi National Accelerator Laboratory, Batavia, Illinois 60510

⁸ Laboratori Nazionali di Frascati, Istituto Nazionale di Fisica Nucleare, I-00044 Frascati, Italy

⁹ Harvard University, Cambridge, Massachusetts 02138

¹⁰ Hiroshima University, Higashi-Hiroshima 724, Japan

¹¹ University of Illinois, Urbana, Illinois 61801

¹² Institute of Particle Physics, McGill University, Montreal H3A 2T8, and University of

- Toronto, Toronto M5S 1A7, Canada*
- ¹³ *The Johns Hopkins University, Baltimore, Maryland 21218*
- ¹⁴ *National Laboratory for High Energy Physics (KEK), Tsukuba, Ibaraki 305, Japan*
- ¹⁵ *Lawrence Berkeley Laboratory, Berkeley, California 94720*
- ¹⁶ *Massachusetts Institute of Technology, Cambridge, Massachusetts 02139*
- ¹⁷ *University of Michigan, Ann Arbor, Michigan 48109*
- ¹⁸ *Michigan State University, East Lansing, Michigan 48824*
- ¹⁹ *University of New Mexico, Albuquerque, New Mexico 87131*
- ²⁰ *Osaka City University, Osaka 588, Japan*
- ²¹ *Universita di Padova, Istituto Nazionale di Fisica Nucleare, Sezione di Padova, I-35131
Padova, Italy*
- ²² *University of Pennsylvania, Philadelphia, Pennsylvania 19104*
- ²³ *Istituto Nazionale di Fisica Nucleare, University and Scuola Normale Superiore of Pisa,
I-56100 Pisa, Italy*
- ²⁴ *University of Pittsburgh, Pittsburgh, Pennsylvania 15260*
- ²⁵ *Purdue University, West Lafayette, Indiana 47907*
- ²⁶ *University of Rochester, Rochester, New York 14627*
- ²⁷ *Rockefeller University, New York, New York 10021*
- ²⁸ *Rutgers University, Piscataway, New Jersey 08854*
- ²⁹ *Academia Sinica, Taipei, Taiwan 11529, Republic of China*
- ³⁰ *Texas A&M University, College Station, Texas 77843*
- ³¹ *Texas Tech University, Lubbock, Texas 79409*
- ³² *University of Tsukuba, Tsukuba, Ibaraki 305, Japan*
- ³³ *Tufts University, Medford, Massachusetts 02155*
- ³⁴ *University of Wisconsin, Madison, Wisconsin 53706*
- ³⁵ *Yale University, New Haven, Connecticut 06511*
- (September 19, 2018)

Abstract

We present a study of events with Z bosons and hadronic jets produced in $\bar{p}p$ collisions at a center-of-mass energy of 1.8 TeV. The data consist of 6708 $Z \rightarrow e^+e^-$ decays from 106 pb⁻¹ of integrated luminosity collected using the CDF detector at the Tevatron Collider. The $Z + \geq n$ jet cross sections and jet production properties have been measured for $n = 1$ to 4. The data compare well to predictions of leading order QCD matrix element calculations with added gluon radiation and simulated parton fragmentation.

PACS numbers: 14.70

The Z boson was discovered in $\bar{p}p$ collisions at CERN in 1983 [1,2]. Since then, the hadronic production properties of the Z have been studied using relatively small event samples, most recently from experiments at the Fermilab Tevatron Collider [3]. In this Letter we describe an extension of these studies based on a much larger sample of 6708 $Z \rightarrow e^+e^-$ decays obtained from 106 pb⁻¹ of integrated $\bar{p}p$ luminosity using the CDF detector. This event sample is large enough to study the production properties of high energy hadronic jets associated with Z boson production. The $\bar{p}p \rightarrow Z + \text{jet}$ events provide a good test of Quantum Chromodynamics (QCD) calculations since the event sample has very small background and the presence of the Z selects high Q^2 parton-level processes. A determination of the reliability of QCD calculations for heavy boson production is important for verifying the direct W boson backgrounds to top quark production [4,5]. Z boson events are free of top quark contamination and provide a clean test of Standard Model heavy boson production. As part of this study we examine the Z boson sample for evidence of excess b quark decays that could indicate new particle production.

The elements of the CDF detector of primary importance to this analysis are the central tracking chamber (CTC), the calorimeters, and the silicon vertex detector (SVX). The CTC, which is immersed in a 1.4 T solenoidal magnetic field, measures the momenta and trajectories of charged particles in the region $|\eta| < 1.1$ (where $\eta = -\ln(\tan(\theta/2))$) [6]. The calorimeters are divided into electromagnetic and hadronic components and cover the pseudorapidity range $|\eta| < 4.2$. The four-layer silicon strip detector (SVX) [7], located just outside the beampipe, provides precise tracking in the plane transverse to the beam direction and is used to reconstruct secondary decay vertices from B hadrons. The CDF detector is described in detail elsewhere [4,8].

Events with Z bosons are identified by looking for the decay $Z \rightarrow e^+e^-$. We demand that candidate events pass a high- E_T electron trigger. The event selection requires an isolated electron [9] that satisfies tight selection cuts [10] and has a track in the central region ($|\eta| \leq 1.1$). Events containing a central electron with transverse energy $E_T \geq 20$ GeV are required to have a second electron that satisfies looser selection cuts and has opposite charge where the sign of the track curvature is well-measured. The second electron is detected in either the central calorimeter ($E_T \geq 20$ GeV and $|\eta| \leq 1.1$), the plug calorimeter ($E_T \geq 15$ GeV and $1.1 \leq |\eta| \leq 2.4$), or the forward calorimeter ($E_T \geq 10$ GeV and $2.4 \leq |\eta| \leq 3.7$). We remove electrons with photon conversion characteristics. The separation in $\eta-\phi$ between the centroid of an electron calorimeter cluster and that of any jet in the event, measured in $\Delta R = \sqrt{\Delta\eta^2 + \Delta\phi^2}$, must exceed $\Delta R = 0.52$.

An event sample of 6708 $Z \rightarrow e^+e^-$ decays is selected by requiring the electron pair masses to be within 15 GeV/ c^2 of the nominal Z boson mass of 91 GeV/ c^2 . The background in these data and the $Z \rightarrow e^+e^-$ acceptance due to our selection cuts are measured as a function of associated jet multiplicity as described below.

Hadronic jets produced in association with the Z bosons are selected using a clustering algorithm [11] with a cone size of $R_j = 0.4$. The jet energies are corrected to account for variations in calorimeter response, estimates of fragmentation energy outside the jet cone, and underlying event energy within the jet cone. Initially, we consider all jets with corrected transverse energy $E_T \geq 12$ GeV. When the separation between two jets is less than $\Delta R = 0.52$, they are combined vectorially into a single jet. The requirements $E_T \geq 15$ GeV and $|\eta| \leq 2.4$ are applied to obtain the hadronic jets used for this analysis. In our sample

of 6708 Z events, 1310 have ≥ 1 jet, 279 have ≥ 2 jets, 57 have ≥ 3 jets, and 11 have ≥ 4 jets. We correct these jet multiplicities for two additional effects: photons counted as hadronic jets, and jets produced in extra $\bar{p}p$ interactions that occur in the same bunch crossing as the Z event. A Z + photon Monte Carlo calculation [12] with detector simulation yields a correction varying from -2% to -3% for photons as a function of jet multiplicity. Using minimum bias events, we estimate the number of jets from additional interactions that pass the selection cuts, and obtain corrections varying from -3% to -5% .

The backgrounds to the Z boson are dominated by jets faking electrons, but include some contributions from heavy quark, $W \rightarrow e\nu + \text{jet}$, and $Z \rightarrow \tau^+\tau^-$ decays. To measure the background we employ a data sample in which all Z boson selection cuts have been applied, except the mass window and electron isolation cuts. By selecting events from this sample in which neither electron candidate is isolated, we obtain a set of events that is almost entirely background with no measurable contribution from $Z \rightarrow e^+e^-$. The mass distribution for these background events is independent of electron candidate isolation. This allows us to estimate the number of background events with isolated electrons that lie within the mass window. This method yields background estimates in the Z boson event sample that are small even at high jet multiplicities. The 1σ upper limits for the backgrounds are 1.1%, 2.3%, 3.0%, and 4.0% for the $n \geq 0, 1, 2,$ and 3 jet events, respectively.

The acceptance for the electrons from a Z boson decay to pass all selection cuts has been measured as a function of the number of associated hadronic jets. Losses due to the electron E_T cuts and detector geometric acceptance requirements have been studied using an inclusive Z boson production model and a leading-order Z + jets QCD calculation [13]. The loss of electrons due to overlap with hadronic jets is determined directly from the data by taking $Z \rightarrow e^+e^-$ events and using a Monte Carlo program to re-decay the Z bosons. The efficiency for decay electrons to be separated from jets and to be isolated sufficiently from other energy in the calorimeters is determined as a function of jet multiplicity. The systematic uncertainties in the overlap efficiencies are determined by varying the polarization of the Z and the separation between the electrons and any jets in the event. For electrons passing the E_T , geometric acceptance, and electron-jet separation cuts, a final acceptance correction is made for electron identification cuts and the efficiency of the online trigger, which selects a high- E_T central electron. The total $Z \rightarrow e^+e^-$ detection efficiencies vary from $(37.3 \pm 0.7)\%$ for Z bosons without jets to $(31.5 \pm 1.4)\%$ for Z bosons with ≥ 4 jets.

The systematic uncertainties on the number of jets due to the jet selection cuts are determined by varying the jet energy scale by $\pm 5\%$, the $|\eta|$ cut by ± 0.2 , the underlying event correction by $\pm 50\%$, the photon removal correction by $\pm 15\%$, and the probability of jets from additional $\bar{p}p$ interactions by $\pm 100\%$. The total jet-counting uncertainties are found to range between 11% for the ≥ 1 jet to 23% for the ≥ 4 jet sample. These errors dominate the uncertainties in the cross section measurements, except for $Z + \geq 4$ jet events where the statistical error is larger.

We measure the cross section for Z production as a function of jet multiplicity using the ratio of the number of detected Z events with $\geq n$ jets to the total number of detected Z events. The cross sections are then determined from this ratio using the inclusive Z boson cross section of 231 ± 12 pb [14] and the ratios of detection efficiencies. This method takes advantage of the cancellation of some systematic uncertainties in the ratios, and gives the most accurate relative $Z + \geq n$ jet cross sections. The measured cross sections for Z

$+ \geq n$ ($n = 1$ to 4) jet events are given in Table I, as are the measured ratios of $\sigma(Z + \geq n \text{ jets})/\sigma(Z + \geq n - 1 \text{ jets})$, which are constant at ~ 0.2 for $n = 1$ to 4 .

The measured cross sections and the production characteristics of the hadronic jets can be compared to QCD calculations. The leading-order matrix element calculations for $Z + n$ parton events (for $n = 1, 2, 3$) are obtained with the VECBOS [13] Monte Carlo program [15]. We use both MRSA and CTEQ3M parton distribution functions, the two-loop α_s evolution, and factorization and renormalization scales varying from $Q^2 = M_Z^2 + p_{T_Z}^2$ of the Z boson to $Q^2 = \langle p_T \rangle^2$, where $\langle p_T \rangle$ is the average p_T of the generated partons. The QCD predictions are indistinguishable for the two parton distribution functions within the statistical uncertainties of our calculation.

The QCD-predicted $Z + \text{jet}$ events are obtained from the parton-level events by including gluon radiation and hadronic fragmentation using the HERWIG [16,17] shower simulation algorithm [18]. This procedure represents a partial higher-order correction to tree-level diagrams. The Z boson events with hadron showers are then introduced into a full CDF detector simulation, and the resulting jets are identified and selected in a manner identical to the data. This procedure allows us to make direct comparisons between the QCD predictions and data.

The Monte Carlo events passing our jet selection cuts are used to determine QCD-predicted cross sections that are compared to the experimental measurements corrected for $Z \rightarrow e^+e^-$ decay losses and backgrounds. These calculated QCD cross sections are given in Table I, and compared to the data via ratios of the measured to QCD-predicted cross sections. Figure 1 shows a plot of the measured cross sections for $Z + \geq n$ jets as a function of n , with the QCD predictions resulting from variations in Q^2 indicated by a superimposed band. For $Q^2 = \langle p_T \rangle^2$, the measured $Z + \geq n$ jet cross sections range from 0.83 to 1.29 times the leading-order QCD predictions. For $Q^2 = M_Z^2 + p_{T_Z}^2$, the ratios of cross sections to leading-order QCD predictions for each n are larger, but nearly constant at 1.7.

In comparing the jet production properties of $Z + \text{jets}$ events, we use the same Monte Carlo event generation described above but apply both $Z \rightarrow e^+e^-$ and jet selection cuts. For this study the QCD-predicted event distributions with $Q^2 = \langle p_T \rangle^2$ are normalized to the number of events in the data samples. Corrections are made for photons counted as hadronic jets and for jets from extra $\bar{p}p$ interactions in the same crossing as the Z event, but no corrections are made for the very small Z boson backgrounds. Figure 2 shows the E_T spectra for the first, second, and third jets (ordered by decreasing E_T) in the ≥ 1 , ≥ 2 , and ≥ 3 jet Z events, respectively. In the $Z + \geq 1$ jet event sample we measure the angle Θ^* between the Z boson and the average beam direction in the $Z + \text{leading jet}$ center-of-mass frame. The distribution of the quantity $|\cos \Theta^*|$, for the range $|\cos \Theta^*| < 0.95$, is shown in Figure 3. In events with two or more jets, we measure the separation in $\eta - \phi$ space between the two leading jets. The resulting ΔR_{jj} distribution is given in Figure 4. This distribution is not corrected for the small number of photons counted as hadronic jets.

The measured jet production properties agree well with the QCD predictions. The χ^2 per degree of freedom is 16.1/18 for the $\cos \Theta^*$ distribution shown in Figure 3 and 7.8/7 for the ΔR_{jj} distribution shown in Figure 4. The QCD-predicted ΔR_{jj} distribution is sensitive to the manner in which gluon radiation is added by the HERWIG algorithm to the VECBOS matrix element, and limiting this radiation results in poorer agreement with the data. The E_T distributions shown in Figure 2 are also in reasonable agreement with the

QCD predictions. The values of the χ^2 per degree of freedom are 19.8/12, 3.7/4, and 6.2/2 for the jet E_T spectra shown in Figures 2a, 2b, and 2c, respectively.

The $Z + \text{jets}$ data sample has been examined for secondary vertices that are characteristic of b quark decays. The secondary vertices are measured using the SVX detector and are reconstructed using the same secondary vertex algorithm developed by CDF and used in the top quark search [4,5]. Of the 1665 jets in the sample, 442 are candidates for secondary vertex reconstruction, which means that they have at least two tracks in the SVX, an uncorrected jet $E_T > 15$ GeV, and $|\eta| < 2$. A control sample of inclusive jet events is used to determine the number of secondary vertices expected from jets in QCD events with no heavy boson. In all, six secondary vertex candidates are found in the data sample where 6.3 ± 1.0 are expected, so there is no excess of b quark decays over the expected number in this $Z + \text{jets}$ dataset.

In summary, this Letter contains an analysis of jet production properties associated with $Z \rightarrow e^+e^-$ events selected from 106 pb^{-1} of $\bar{p}p$ collisions at a center-of-mass energy of 1.8 TeV. Comparisons are made between the data and leading order parton matrix elements with HERWIG-simulated parton shower and fragmentation. The ratios of the measured to QCD-predicted cross sections are found to vary from 1.29 ± 0.17 to 1.69 ± 0.22 for $\bar{p}p \rightarrow Z + \geq 1 \text{ jet}$ when the Q^2 scale is varied from $\langle p_T \rangle^2$ to $M_Z^2 + p_{T_Z}^2$. The QCD-predicted jet production properties are in generally good agreement with the measured distributions. The incidence of b quark decays in the jets associated with Z bosons is consistent with that observed in similar jets from events with no heavy boson.

We thank the Fermilab staff and the technical staffs of the participating institutions for their vital contributions. We also thank Walter Giele and the theory group at the University of Durham for many useful discussions. This work was supported by the U.S. Department of Energy and National Science Foundation; the Italian Istituto Nazionale di Fisica Nucleare; the Ministry of Education, Science and Culture of Japan; the Natural Sciences and Engineering Research Council of Canada; the National Science Council of the Republic of China; and the A. P. Sloan Foundation.

REFERENCES

- [1] G. Arnison *et al.*, Phys. Lett. B **126**, 398 (1983).
- [2] P. Bagnaia *et al.*, Phys. Lett. B **129**, 130 (1983).
- [3] F. Abe *et al.*, Phys. Rev. Lett. **67**, 2937 (1991).
- [4] F. Abe *et al.*, Phys. Rev. D **50**, 2966 (1994).
- [5] F. Abe *et al.*, Phys. Rev. Lett. **74**, 2626 (1995).
- [6] We use a polar coordinate system in which z is along the proton direction, ϕ is the azimuthal angle, and θ is the polar angle. Pseudorapidity (η) is calculated using $z = 0$ at the center of the detector for fiducial cuts and at the interaction point for event variables (i.e. ΔR cones).
- [7] D. Amidei *et al.*, Nucl. Instrum. Methods **A350**, 73 (1994).
- [8] F. Abe *et al.*, Nucl. Instrum. Methods **A271**, 387 (1988).
- [9] An isolated electron is defined to be one for which the transverse calorimeter energy in the cone of radius 0.4 in $\eta - \phi$ space around the electron cluster is less than 10% of the electron transverse energy.
- [10] F. Abe *et al.*, Phys. Rev. D **44**, 29 (1991). Differences in our selection cuts from those described in this reference are that we use (i) $0.5 < E/p < 2.0$ and (ii) $\chi_{strip}^2 < 10$.
- [11] F. Abe *et al.*, Phys. Rev. D **45**, 1448 (1992).
- [12] U. Baur and E.L. Berger, Phys. Rev. D **47**, 4889 (1993).
- [13] F.A. Berends, W.T. Giele, H. Kuijff, and B. Tausk, Nucl. Phys. B **357**, 32 (1991).
- [14] F. Abe *et al.*, Fermilab-Pub-95/301-E (1995). Submitted to Phys. Rev. Lett.
- [15] We generate $Z + \text{parton}$ events with parton $p_T > 8 \text{ GeV}/c$, $|\eta| < 3.5$, and $\Delta R > 0.4$ between partons.
- [16] G. Marchesini and B. Webber, Nucl. Phys. B **310**, 461 (1988).
- [17] G. Marchesini *et al.*, Comput. Phys. Comm. **67**, 465 (1992).
- [18] The HERWIG initial state radiation contributes jets to the Z boson event. For the purpose of the calculation presented here, a kinematic limit of $\sqrt{M_Z^2 + p_{Tz}^2}$ is applied to the HERWIG gluon radiation.

FIGURES

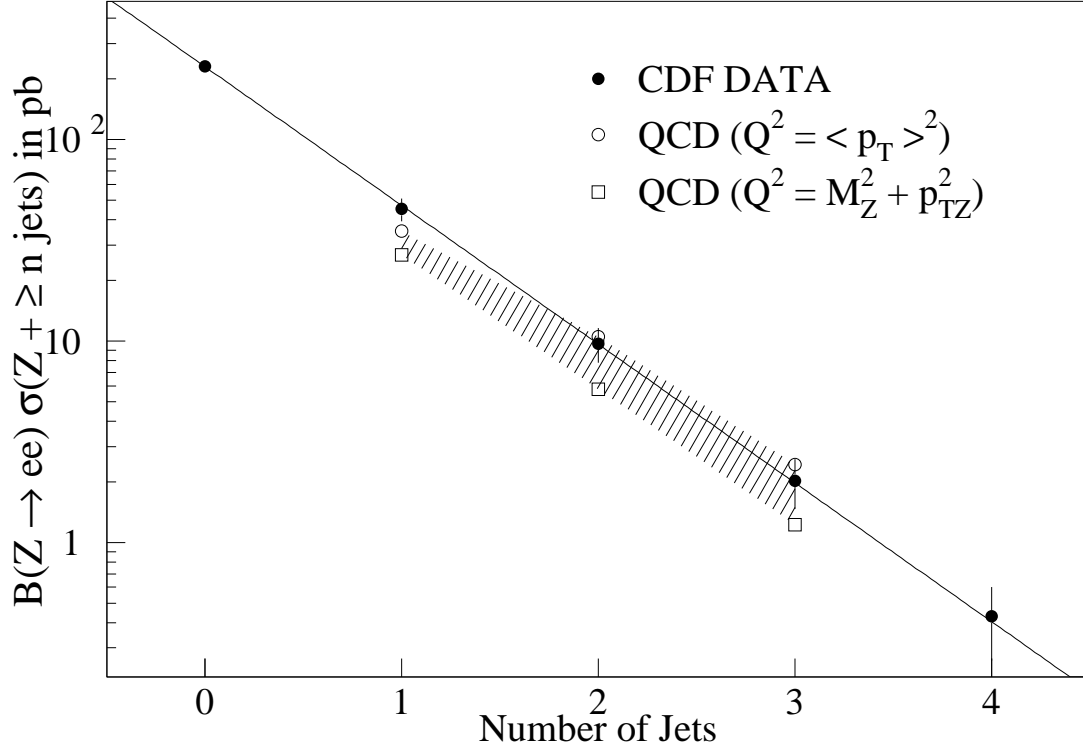


FIG. 1. Cross section for $Z + \geq n$ jets versus n , where $Z \rightarrow e^+e^-$. The QCD prediction band is determined by using two different renormalization scales. The solid line is an exponential fit to the measured cross sections. The error bars include statistical and systematic uncertainties.

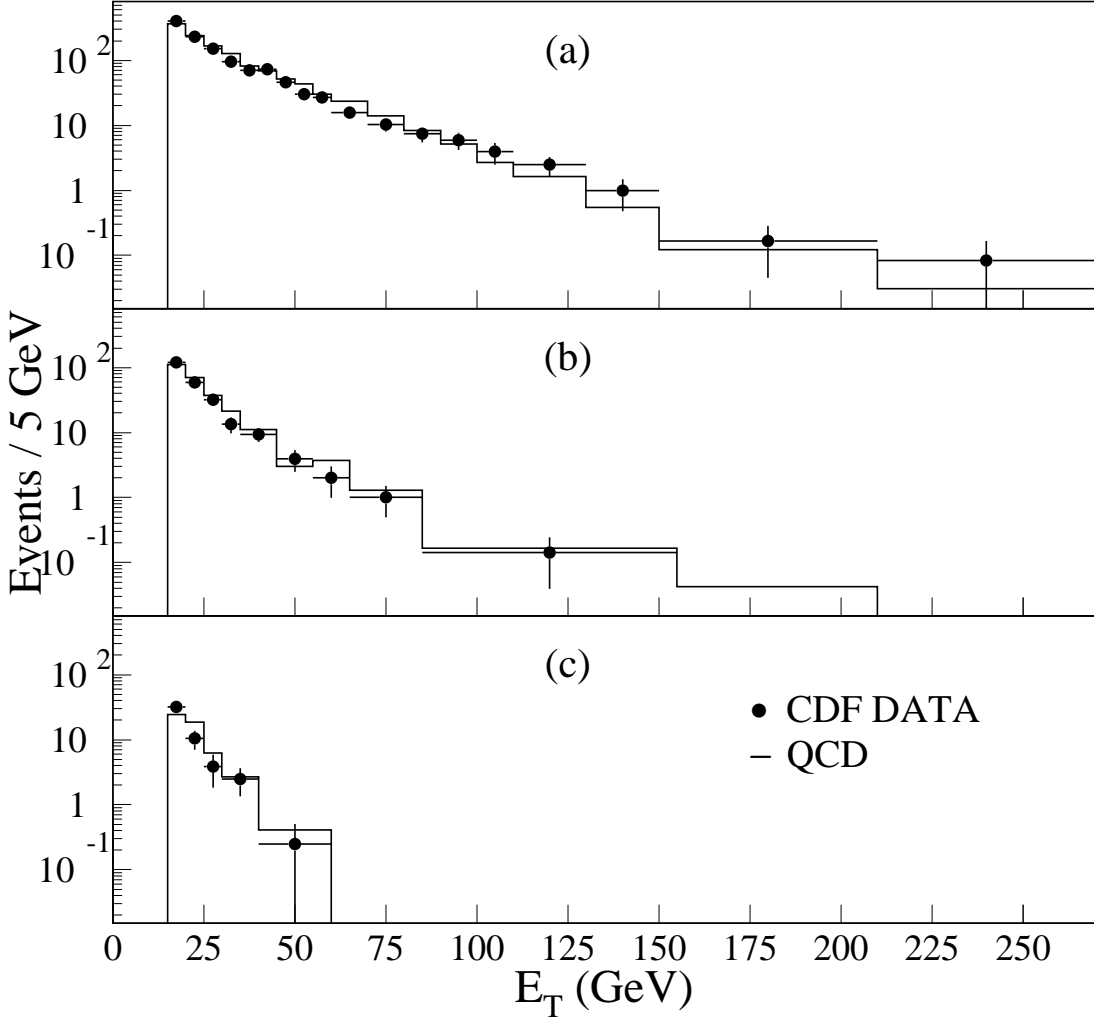


FIG. 2. Transverse energy of the (a) first, (b) second, and (c) third highest E_T jets in ≥ 1 , ≥ 2 , and ≥ 3 jet events, respectively. The points are the data with statistical errors only, and the solid histograms are the QCD predictions (normalized to the data) described in the text.

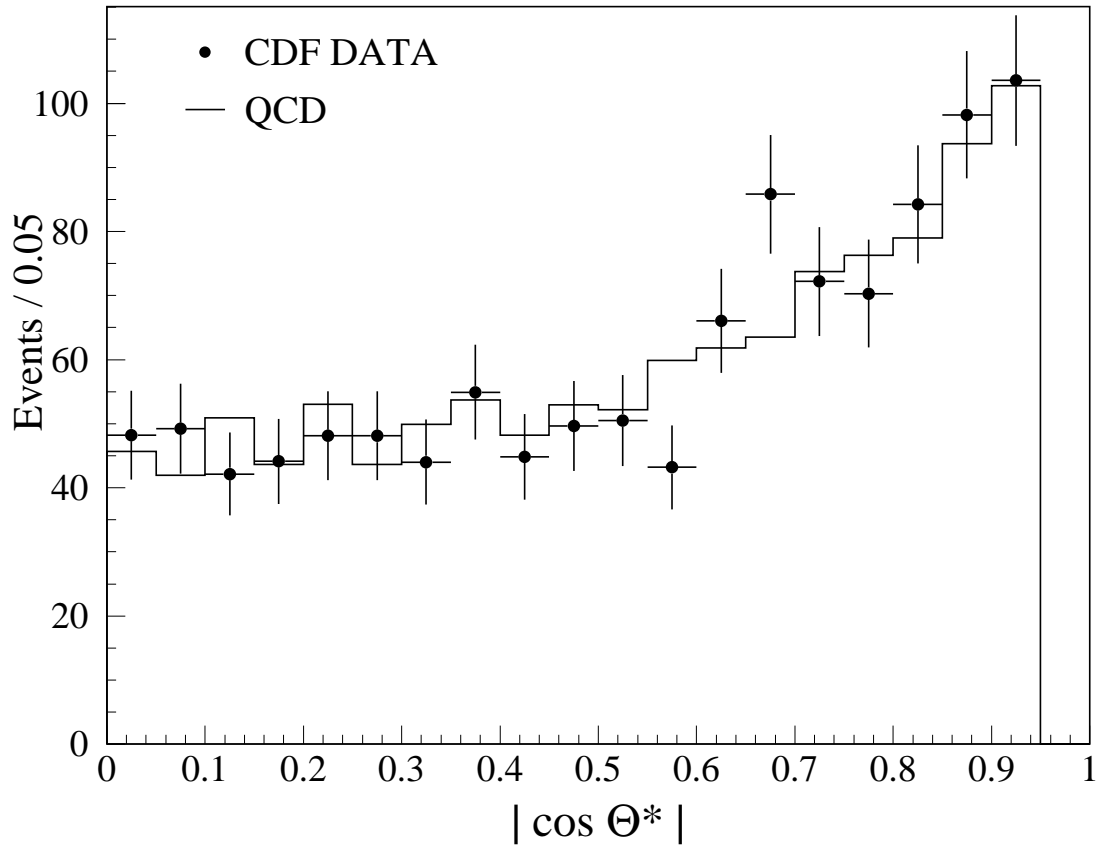


FIG. 3. The $|\cos \Theta^*|$ distribution of the Z in ≥ 1 jet events. The angle Θ^* is the angle of the Z measured with respect to the average beam direction in the $Z +$ leading jet center-of-mass frame. The Monte Carlo predictions are normalized to the data, and the data errors are statistical only.

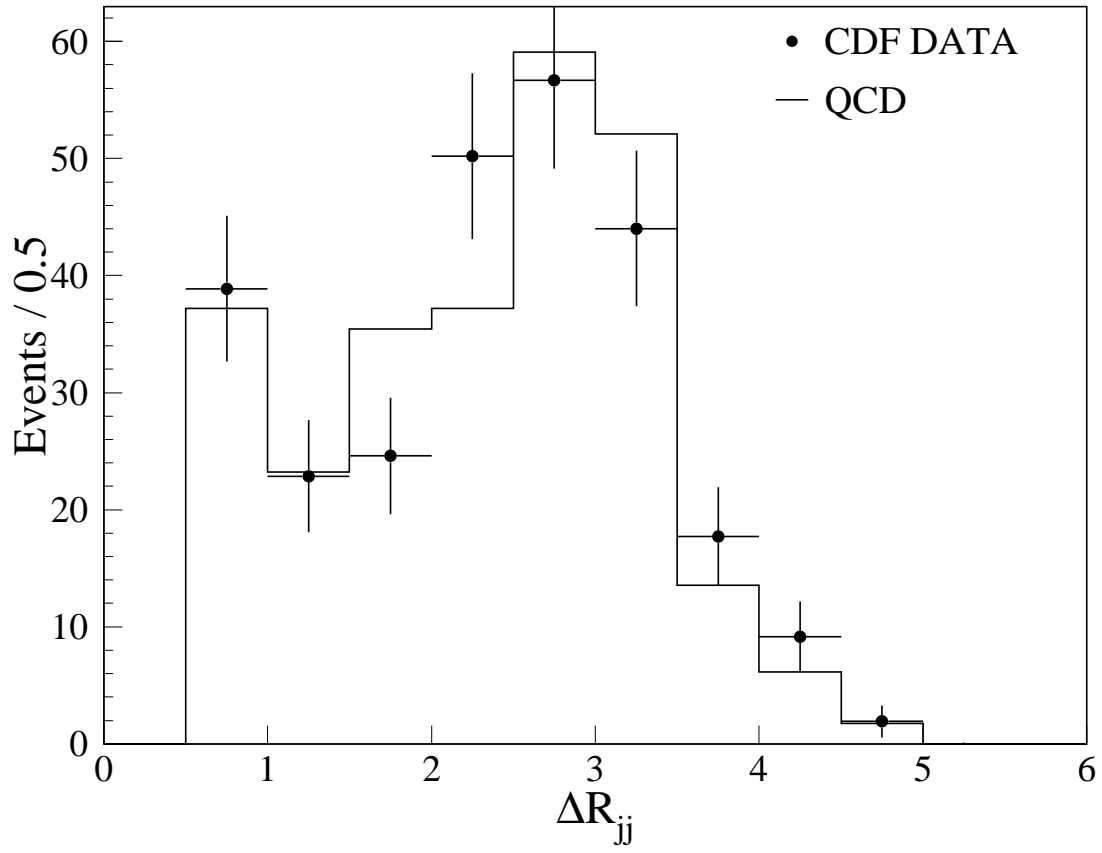


FIG. 4. Separation in $\eta - \phi$ space between the two leading jets in $Z + \geq 2$ jet events. The Monte Carlo predictions are normalized to the data. The data errors are statistical only.

TABLES

n Jets	$BR \times \sigma_{\text{Data}}$ (pb)	$Q^2 = \langle p_T \rangle^2$		$Q^2 = M_Z^2 + p_{T_Z}^2$		$\sigma(n)/\sigma(n-1)$ (Data)
		$BR \cdot \sigma_{\text{QCD}}(\text{pb})$	$\sigma_{\text{Data}}/\sigma_{\text{QCD}}$	$BR \cdot \sigma_{\text{QCD}}(\text{pb})$	$\sigma_{\text{Data}}/\sigma_{\text{QCD}}$	
≥ 0	$231 \pm 6 \pm 11$	—	—	223 ± 10	1.04 ± 0.07	—
≥ 1	$45.2 \pm 1.2 \pm 5.7$	35.16 ± 0.54	1.29 ± 0.17	26.82 ± 0.40	1.69 ± 0.22	0.196 ± 0.007
≥ 2	$9.7 \pm 0.6 \pm 1.8$	10.53 ± 0.38	0.92 ± 0.19	5.77 ± 0.16	1.68 ± 0.34	0.215 ± 0.014
≥ 3	$2.03 \pm 0.28 \pm 0.49$	2.44 ± 0.17	0.83 ± 0.24	1.23 ± 0.08	1.66 ± 0.47	0.210 ± 0.027
≥ 4	$0.43 \pm 0.13 \pm 0.11$					0.211 ± 0.059

TABLE I. $Z + \geq n$ jet Cross Sections. The first error on the data cross sections is the statistical error; the second includes the systematic error on the Z acceptance and the luminosity error added in quadrature. For $n = 1$ to 4, the second error also includes the jet-counting uncertainty, as described in the text. The leading order (LO) Monte Carlo cross sections are generated with VECBOS for Q^2 scales of $\langle p_T \rangle^2$ and $M_Z^2 + p_{T_Z}^2$. The ≥ 0 jet calculation is next-to-next-to-leading order (NNLO) with $Q^2 = M_Z^2$. The error on the NNLO QCD cross section includes systematic and statistical uncertainties; for the LO cross sections the errors are statistical.